

Supporting Information

Anion Species Dependence of Undetected Water Molecules along the Hofmeister Series in Various Lithium Electrolytes

Using Near-infrared and Nuclear Magnetic Resonance Spectroscopy

Jingchao XU,[§] Youngchol KOH, Shinya TAKAYOSE, Hideshi MAKI,^{*,§§}

and

Minoru MIZUHATA^{*, §§§}

Department of Chemical Science and Engineering, Graduate School of Engineering,

Kobe University, 1-1 Rokkodai-cho, Nada-ku, Kobe 657-8501, Japan

** Corresponding author: mizuhata@kobe-u.ac.jp*

maki@kobe-u.ac.jp

[†]A part of this paper has been presented in the 102nd CSJ Annual Meeting in 2022 (Presentation #A202-1vn-05) and the 2022 ECSJ Fall Meeting (Presentation #2P15)

§ ECSJ Student Member

§§ ECSJ Active Member

§§§ ECSJ Fellow

ORCID J. Xu: 0009-0007-3697-0497

M. Maki: 0000-0002-8960-4833

M. Mizuhata: 0000-0002-4496-2215

S1. NIR Measurement for Fumed Silica/ Typical Solvents Coexisting Systems for Validation of the Quantitative Detection Capability

S1. 1 Experimental

To confirm the quantitative accuracy of the transmission spectrum measurements, NIR spectra was measured on samples in which SiO₂ powder and various kinds of the liquid compounds for electrolyte solvents were physically mixed.

Fumed silica (Nippon Aerosil Co., Ltd., AEROSIL 200F) was prepared as the solid phase. The fumed silica was dried in a muffle furnace at 800 °C and brought down to room temperature in a desiccator in vacuum. The dried fumed silica was stored in a glove box in Ar atmosphere. The particle size of the dried silica was characterized by Field Emission Scanning Electron Microscope (FE-SEM, JEM-6335F, JEOL Ltd.), as shown in Fig. S1.

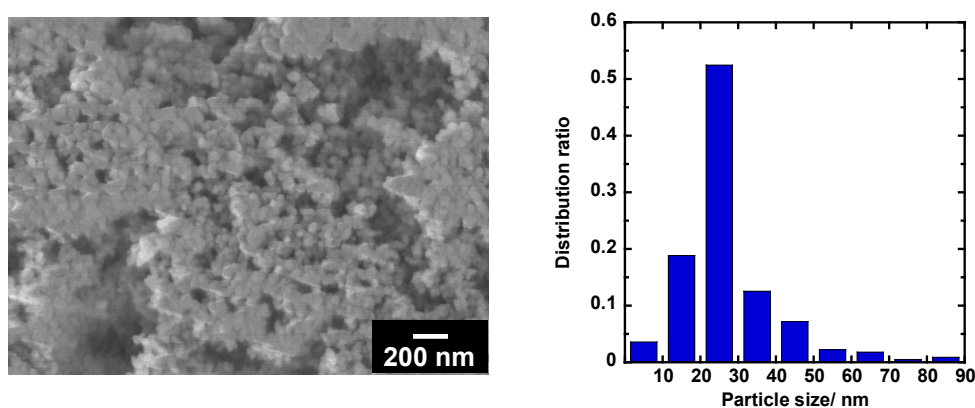


Figure S1. Characterization of fumed SiO₂. (a) SEM image of SiO₂ after drying at 800 °C and (b) particle size distribution ratio after drying at 800 °C.

The true density of the SiO₂ particles, ρ , was measured by Archimedeian method using a pycnometer by Eq. S1:

$$\rho = \frac{m_b - m_a}{(m_b - m_a) - (m_c - m_d)} \rho_{\text{water}} \quad (\text{S1})$$

where, m_a : the weight of the empty pycnometer,

m_b : the total weight of the pycnometer with certain amount of silica particles,

m_c : the total weight of the pycnometer with certain amount of silica particles and filled water,

m_d : the total weight of the pycnometer filled water fully,

and ρ_{water} , the density of the water, respectively.

Table S1. Physical properties of fumed SiO₂ as solid phase after drying.

Particle size	34 nm
Density	2.2 g cm ⁻³
Specific surface area	192.6 m ² g ⁻¹

Specific surface area of fumed silica was measured by BET method with Quantachrome Instruments NOVA 2200e. Physical properties of fumed SiO₂ as solid phase after drying are shown in Table S1.

For liquid phase, we used water, Propylene carbonate (PC, Nacalai Tesque Inc.), 1, 2-Dimethoxyethane (DME, Nacalai Tesque Inc.). Deionized distilled water (conductivity < 0.055 $\mu\text{S cm}^{-1}$) was obtained by purification of Advantec RFD240RA. PC and DME were added with molecular sieve to remove the water, and after the water content was tested by Karl Fischer (Mitsubishi Chemical, CA-310) at no more than 15 ppm.

Fumed silica and each liquid samples were mixed in the volume fraction of the liquid phase in an alumina mortar by volume fraction of liquid phase from 80 vol% to 100 vol%), which calculated by following equation:

$$V_s(\text{vol}\%) = \frac{W_l/\rho_l}{W_l/\rho_l + W_s/\rho_s} \times 100 \quad (\text{S2})$$

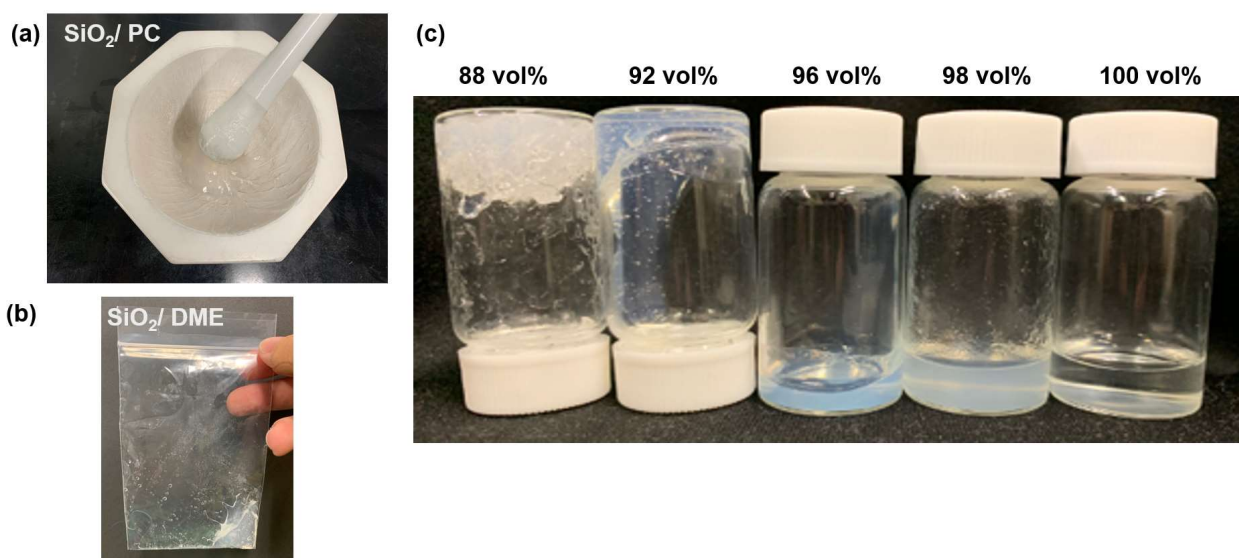


Figure S2. Photos of solid-liquid mixed samples. (a) Homogeneous mixing of PC and fumed SiO₂ using a mortar and pestle; (b) Homogeneously mix DME and SiO₂ in a sealed transparent bag to prevent the evaporation of DME; (c) The states of samples obtained at different mixing ratios in the H₂O/ SiO₂ system. Each liquid content is indicated. All procedures were conducted in an argon-filled glove box when using organic solvents as the liquid phase.

where, W_l , W_s , ρ_l , and ρ_s are the weight of the liquid, the weight of the solid, the density of the liquid, and the density of the solid, respectively. The schematic drawing about solid-liquid mixtures are shown in Fig. S2.

As shown in Fig. S3, the model is the dispersion of a solid particle of radius r filled with liquid in a face-centered cubic arrangement with inter-particle gaps of $2d$. In this case, the average thickness d of the liquid phase is;

$$d = \left(\frac{1}{16\sqrt{2}} V \right)^{\frac{1}{3}} - r = \left[\left(\frac{\pi}{3\sqrt{2} V_s} \right)^{\frac{1}{3}} - 1 \right] r \quad (S3)$$

V is the unit volume of a face-centered cubic arrangement, and V_s is the volume fraction of the solid phase.

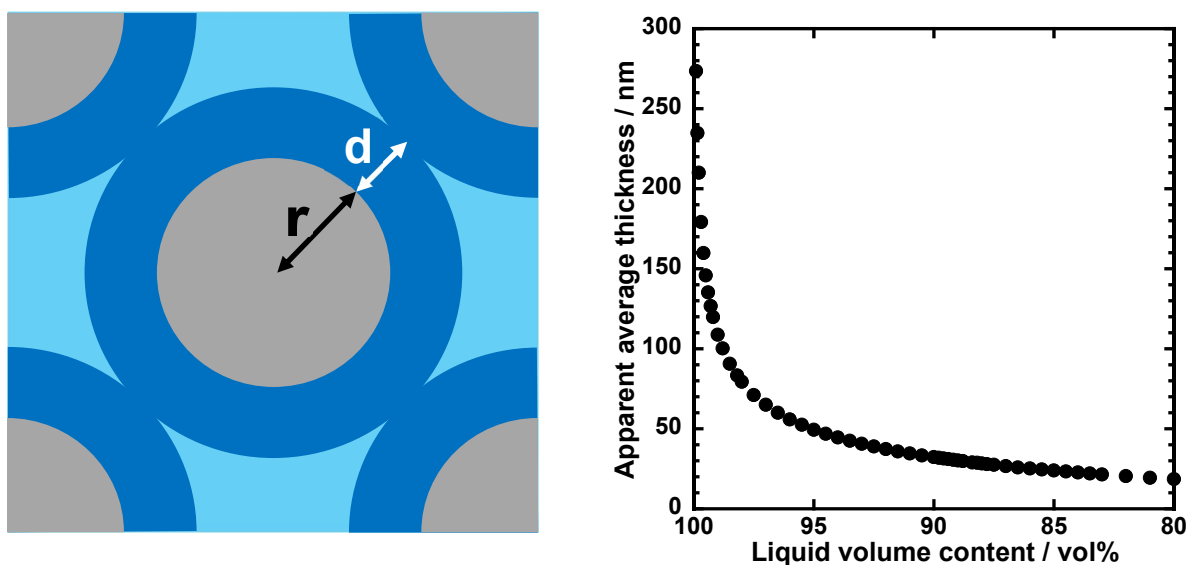


Figure S3. (a) Ideal model for solid-liquid coexistence system. r : radius of SiO_2 particles, d : average liquid phase thickness on the particle surface; (b) Relationship between average thickness of liquid phase and volume fraction of liquid phase.

S1.2 NIR Spectra for Solid/Liquid Coexisting Systems.

In this section, we describe the NIR spectra of solid-liquid coexistent samples containing each solvent and their analysis by the measurement method described in 2.3. The measurement ranges were 1200-2500 nm for aqueous system, 1580-2015 nm for PC system, and 1000-2240 nm for DME system.

The NIR spectra of the samples of H_2O , PC, and DME homogeneously mixed with dried fumed SiO_2 are shown in Fig. S4, where the combination bands of OH symmetric stretching vibration (ν_1) and asymmetric stretching vibration (ν_3) of water are shown in Fig. S4a. The NIR spectra of PC and DME in Fig. S4(b, c) cannot be accurately distinguished from the individual absorbance attributions

due to the lack of relevant literature reports. Therefore, the entire spectral range was integrated in the calculation of integral absorbance. The integral absorbance values of solvent molecules measured at each liquid volume fraction were divided by the absorbance of the pure liquid phase to obtain the detected liquid phase volume fraction. As shown in Fig. S4(d-f). In the ideal result, the detected liquid phase volume fraction decreases proportionally with the reduction in the liquid phase volume fraction in the mixture. Although at liquid phase volume fractions above 98 vol%, the experimental values slightly exceed the ideal values due to sedimentation of the solid phase, the integral absorbance of the NIR obtained with each solvent indicated good quantitation in detecting water present in a given volume.

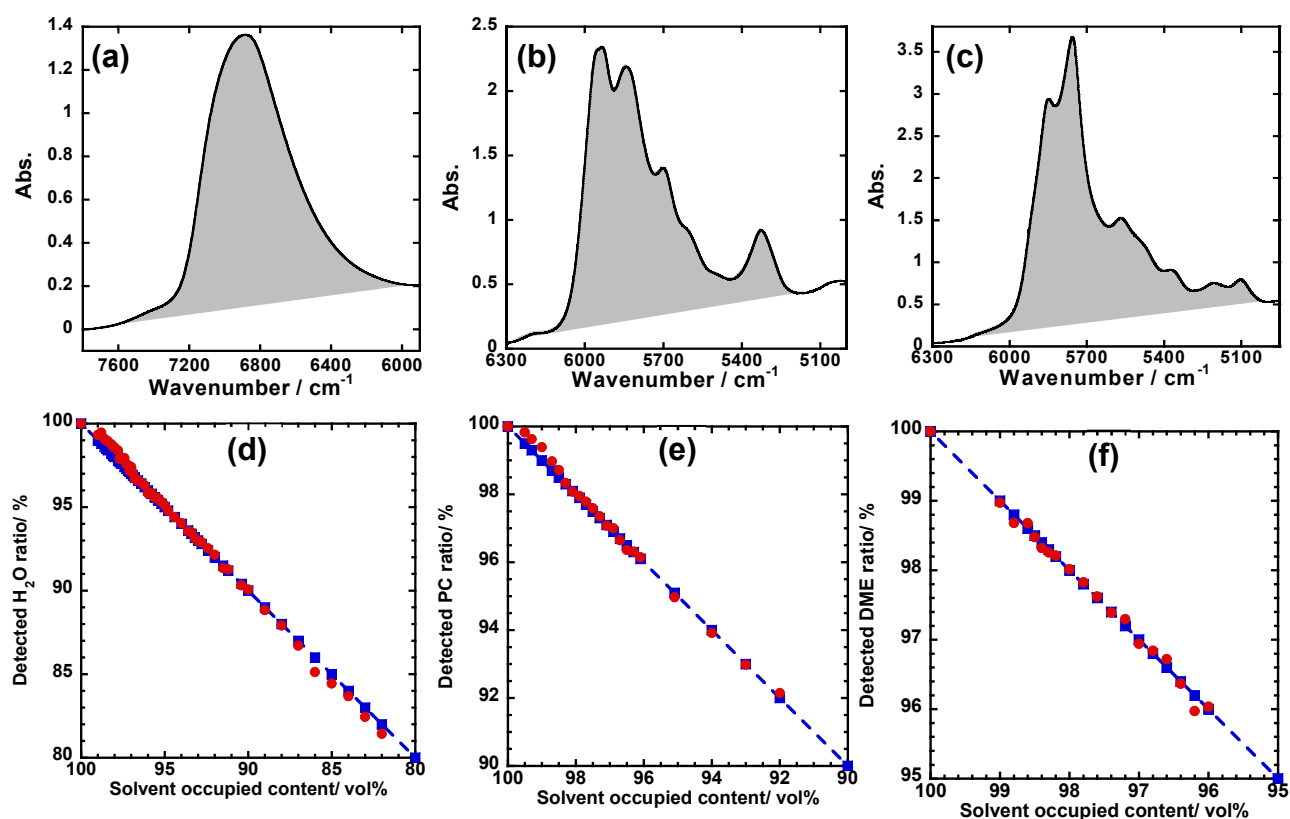


Figure S4. The near-infrared absorption spectra of solvent molecules in a mixed system composed of different solvents and fumed SiO₂ powder, mixed at varying volumetric ratios. a) the combination tone of OH symmetric stretching vibrations and OH asymmetric stretching vibrations of water molecules in bulk water; b) Near infrared absorption peaks of bulk PC; c) Near infrared absorption peaks of bulk DME. By integrating the area of each absorption spectrum (the shaded gray region) to determine the integral absorbance of the solvent molecules and using the peak area of the pure solvent as a reference, we estimated the concentration of solvent molecules in the solid-liquid mixed system based on the ratio of the absorption peak areas, as shown in Figures. d) SiO₂ powder/ H₂O coexisting system, e) SiO₂ powder/ PC coexisting system, and f) SiO₂ powder/ DME coexisting system. In this context, the x-axis represents the actual volumetric fraction of the liquid in the solid-liquid mixed system, while the y-axis indicates the estimated concentration of solvent molecules in the solid-liquid mixture based on calculations. The squares represent ideal results, and the circles represent experimental results.

Similar to the discussion in 3.3 regarding the hydrogen bonding of water molecules in aqueous electrolyte solutions, the results of waveform analysis based on the state of hydrogen bonding are shown in Fig. S5 for solid-liquid coexistent samples. The area ratios of individual absorption bands indicating the state of hydrogen bonding were almost constant from the results for water over the measurement range.

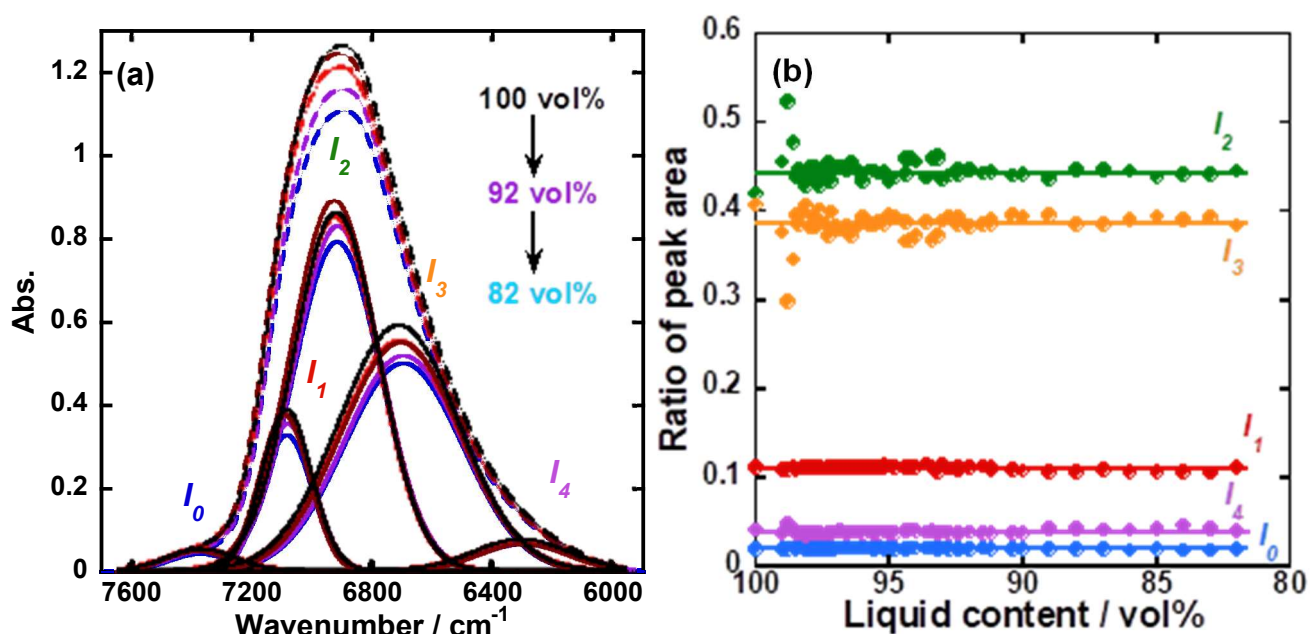


Figure S5. Deconvolution results of the near-infrared absorption spectra of water molecules in SiO₂ powder/ H₂O coexisting system with different mixing ratios. The spectrum colors transition from red to blue, indicating a decreasing volumetric fraction of water in the mixed system. a) NIR spectra of H₂O at different liquid content from 100 vol% (black) to 82 vol% (light blue); b) Variation of the relative area ratio of each Gaussian bands with the volume fraction of the liquid phase in SiO₂ powder/ H₂O coexisting system.

S2. Supplementary materials

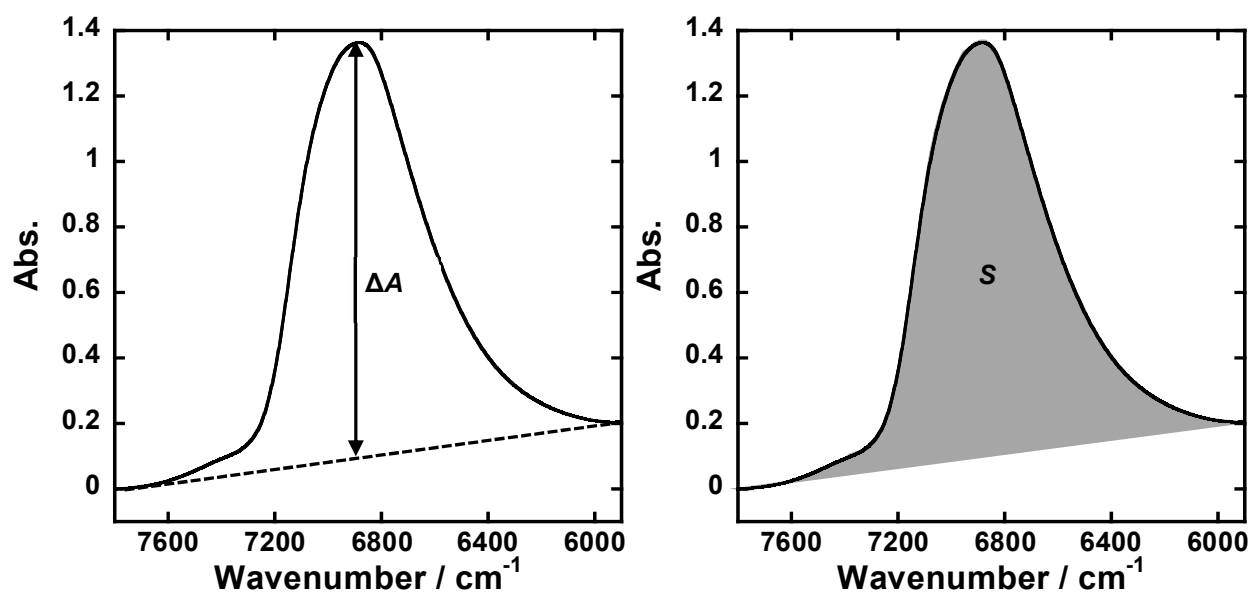


Figure S6. The starting and ending wavenumbers of the near-infrared absorption peaks of water are used to determine the baseline, as shown by the dashed line in the figure. The difference in absorbance between the baseline and the absorption peak at the same wave number is ΔA , as shown in (a). The area of the component between the baseline and the absorption peak is integrated by Eq. 3, and the resulting peak area is used as the integral absorbance S of water over the entire wavelength range.

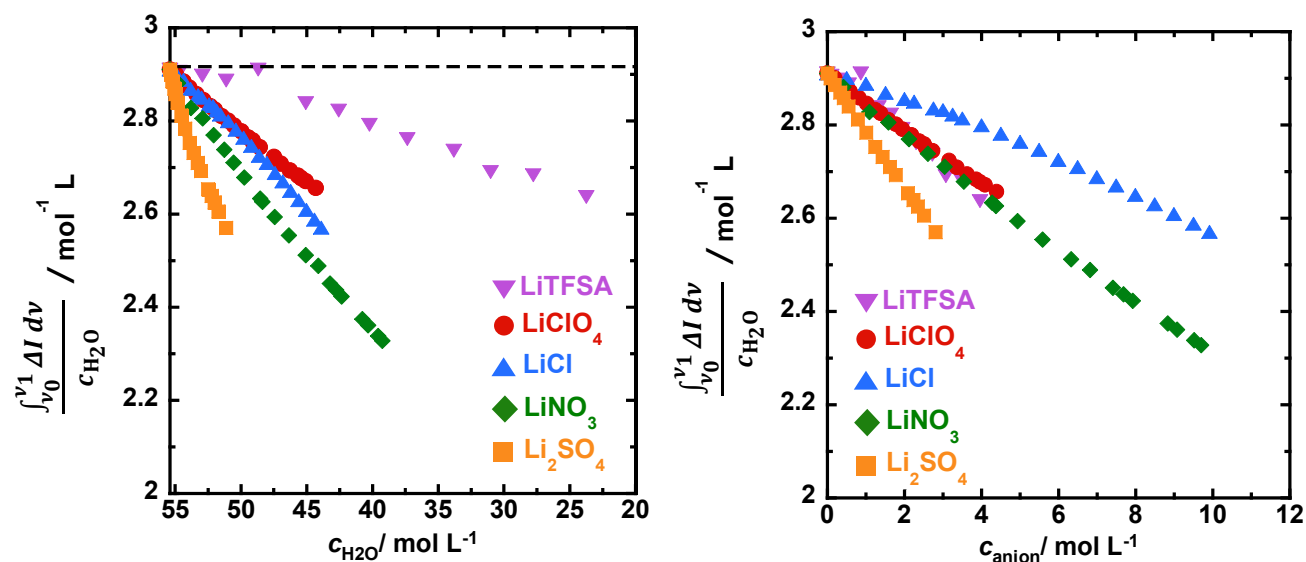


Figure S7. Relationship between the coefficient in Beer's law and (a) the concentration of water in aqueous solution, (b) the concentration of electrolyte in aqueous solution. The dotted line in the figure indicates that ideally, the ratio of absorbance to the concentration of the absorbing substance is a constant value according to Beer's law.

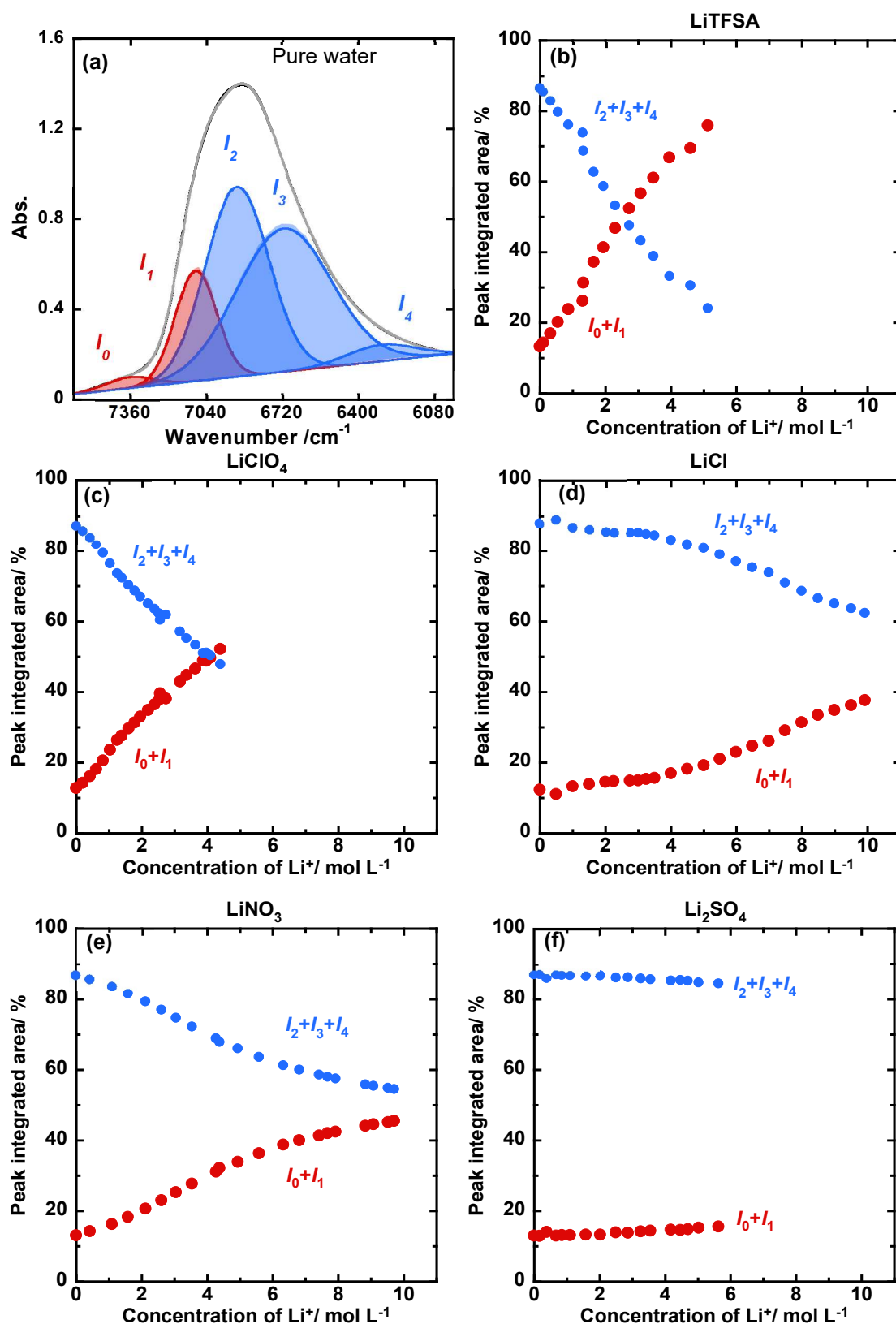


Figure S8. The deconvolution results in aqueous solutions of each Li salt. The five Gaussian components are further categorized into two main groups: I_0+I_1 are water molecules with weak or no hydrogen bonding, while $I_2+I_3+I_4$ are regarded as water molecules with strong hydrogen bonding or forming multiple hydrogen bonds. Changes in the relative occupancy of the two types of water molecules with Li^+ concentration. (b) LiTfSA, (c) LiClO_4 , (d) LiCl, (e) LiNO_3 , (f) Li_2SO_4 .

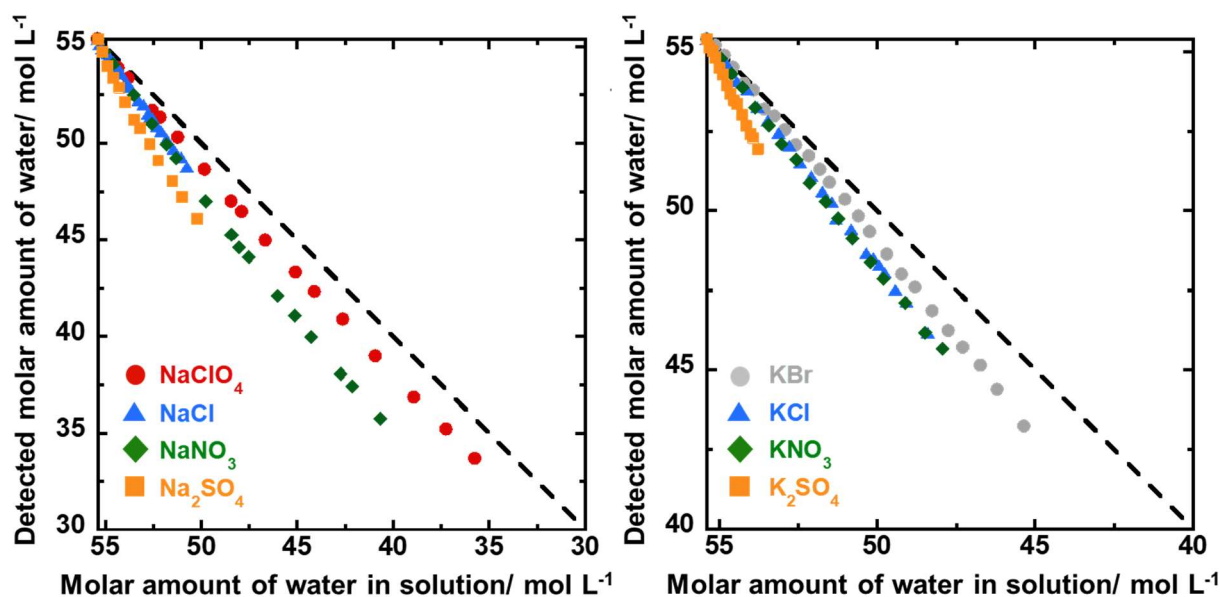


Figure S9. The relationship between the near-infrared detection values of water molecules in alkali metal electrolyte solutions and the actual theoretical values. (a) Water molecule detection rate of Na salts in relation to theoretical values; (b) Water molecule detection rate of K salts in relation to theoretical values. The horizontal axis represents the molar amount of water molecules at different concentrations calculated by Eq. 2', while the vertical axis indicates the molar amount of water molecules detected via near-infrared spectroscopy. The black dashed line in the figure illustrates the ideal scenario in which the number of water molecules measured by near-infrared spectroscopy aligns with the actual number of water molecules present in the solution.